

Magnetic Anisotropy of Quantum Critical Fluctuation in $\text{YBa}_2\text{Cu}_3\text{O}_7$ at High Magnetic Fields of up to 100 T

Shiyue Peng,¹ Xu-Guang Zhou,^{1,*} Yasuhiro H. Matsuda,^{1,†} Qian Chen,¹ Masashi Tokunaga,¹ Yuto Ishii,¹ Satoshi Awaji,² Taiga Kato,³ Tomonori Arita,³ and Yutaka Yoshida³

¹*Institute for Solid State Physics, University of Tokyo, Kashiwa, Chiba 277-8581, Japan*

²*Institute for Materials Research, Tohoku University, Sendai, Miyagi 980-8577, Japan*

³*Department of Electrical Engineering, Nagoya University, Nagoya, Aichi 464-8603, Japan*

The investigation of high-temperature superconductors under high magnetic fields is one of the most important topics in condensed matter physics. For $\text{YBa}_2\text{Cu}_3\text{O}_7$ (YBCO), the measurements of magnetoresistance under a high magnetic field are technically challenging because the required magnetic field (B) is 100 T class. The low temperature (from 52 to 150 K) magnetoresistance is measured in optimally-doped YBCO thin films under the condition $B \parallel \text{CuO}_2$ -plane up to 103 T by employing the single-turn coil technique and a radio frequency reflection method. The electrical resistivity ρ exhibits B -linear behavior in the normal phase in the high magnetic field region. The field slope coefficient β ($=d\rho/dB$) becomes converged at low temperatures. The convergence of β below T_c indicates the field-induced strange metal phase, which is determined by the quantum critical fluctuation at high magnetic fields. The β value difference under the different directions of the magnetic field suggests the strong anisotropy in quantum critical fluctuations in the strange metal phase of YBCO.

Introduction. -High-temperature superconductivity is one of the most important topics in condensed matter physics because it is not only a typical quantum many-body problem [1, 2], but also a problem leading to potentially transformative applications [3–5]. As the high-temperature superconductors (HTSCs) lose their superconductivity with increasing temperature, they enter the metal state. Here, the resistance shows an unusual linear relationship up to 1000 K [6–8], a behavior beyond the scope of traditional Fermi liquid theory [9, 10]. While the exact mechanism of high-temperature superconductivity remains debated, the widely accepted view is that the linear temperature (T) dependence of resistance is directly tied to the superconductivity’s ground state. This characteristic behavior serves as a signature of the strange metal state [11–14].

Similarly, when superconductivity is suppressed by a magnetic field, the system also exhibits the property of the strange metals. In previous studies, Giraldo-Gallo *et al.* have reported that magnetoresistance (MR) of $\text{La}_{2-x}\text{Sr}_x\text{CuO}_4$ (LSCO) under $B \perp \text{CuO}_2$ -plane up to 80 T [15], in which the MR shows the linear-in-field (B -linear) behavior as well as the linear-in-temperature (T -linear) resistivity of the metal phase. Because the coefficients of linear resistance, β ($=d\rho/dB$) and α ($=d\rho/dT$), gradually develop with approaching the critical doping condition in LSCO in a similar manner, these two coefficients are considered to be directly affected by the quantum criticality, and dominate the non-Fermi liquid characteristic of the normal phase together. This relationship between β and α is often pointed in the strange

metal phase [15].

Studies of other cuprate HTSCs under high magnetic fields is helpful to understand the properties of this strange metal phase. $\text{YBa}_2\text{Cu}_3\text{O}_7$ (YBCO) is one of the most attractive HTSCs because of the high critical temperature $T_c \sim 90$ K and its potential applications. The strange metal state in YBCO at low temperatures and high magnetic fields has never been well investigated because ultra-high magnetic fields are required to suppress the superconducting phase [16, 17].

Sekitani *et al.* [17–19] have investigated the $B - T$ phase diagram using the radio frequency (RF) method, and their results suggest that the critical magnetic field B_{c2} at lowest temperatures are approximately 110 and 250 T in $B \perp \text{CuO}_2$ -plane and $B \parallel \text{CuO}_2$ -plane, respectively. This proves the anisotropic critical magnetic fields B_{c2} . Based on the previous studies [20, 21], the B -linear MR is anticipated to appear in YBCO. Furthermore, it is expected to also exhibit anisotropy in the field direction ($B \perp \text{CuO}_2$ -plane or $B \parallel \text{CuO}_2$ -plane) through the two-dimensionality of the conducting CuO_2 -plane under external field above B_c . However, generating such high magnetic fields can only be achieved through a destructive manner [22, 23]. Therefore, due to technical limitations [24], it is challenging to investigate the electronic properties of YBCO in magnetic fields exceeding 100 T.

In this study, we successfully measured the magnetoresistance (MR) of optimally doped YBCO thin films under a magnetic field ($B \parallel \text{CuO}_2$ -plane) up to 103 T. This was accomplished by developing an RF reflection method adapted to a single-turn coil magnetic field generator. MR curves were obtained over a temperature range spanning from 52 to 150 K. Once the superconducting phase is suppressed, the normal phase demonstrates a linear relationship with the magnetic field (B -

* zhou@issp.u-tokyo.ac.jp

† ymatsuda@issp.u-tokyo.ac.jp

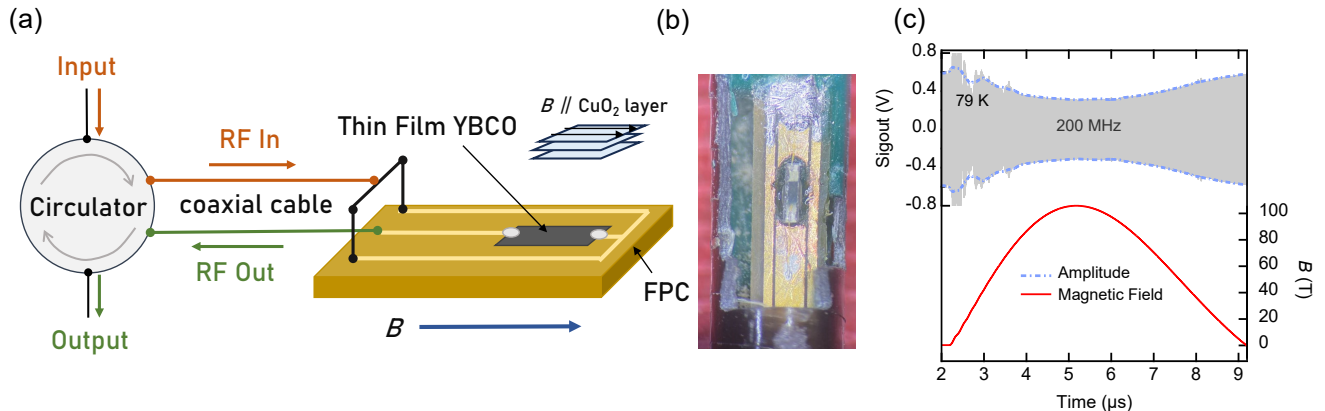


FIG. 1. (a) The schematic diagram of the RF (Radio Frequency) measurement system. (b) A photo of the end of FPC connected with a thin film YBCO sample. (c) The typical raw data of the RF reflection signal at 79 K with its envelope curves together with the magnetic field waveform.

linear behavior) in the high magnetic field region. This behavior underscores the importance of many-body effects arising from strong interactions in what is known as the strange metal [11, 15]. We further analyze the field slope parameter β ($=d\rho/dB$) of the MR curves, finding its value converging below T_c . The magnitude of β is also dependent on the magnetic field direction relative to the CuO_2 -plane, indicating anisotropic quantum critical fluctuations in the strange metal phase. These results are served as a distinctive signature of the strange metal phase near quantum critical points, highlighting the significant role of quantum critical fluctuations in governing superconductivity.

Experiment. -The experiment employs an optimally-doped $\text{YBa}_2\text{Cu}_3\text{O}_7$ thin film sample with a critical temperature T_c of approximately 89 K [25], as illustrated in Fig. S1. The film, with a thickness of 200 nm, is deposited on a SrTiO_3 (100) substrate. To ensure good electrical connectivity, silver is sputtered onto both ends of the sample's surface, connecting it to thin Au wires via silver paste. Pulsed magnetic fields up to 103 T are generated using a destructive method, specifically the vertical-type single-turn coil technique [22]. The magnetic field is applied parallel to the CuO_2 -plane and is also parallel to the thin film, which is (001) oriented, as shown in Fig. 1(a). For impedance measurement, a radio frequency (RF) reflection system is developed.

In Fig 1(a), the RF method is implemented using a circulator, with input, output, and sample ports. The frequency of the RF incident wave is set at 200 MHz (input), which is over two orders of magnitude higher than the pulsed magnetic field waveform frequency (approximately 200 kHz). For the sample port, a 150 mm-long flexible printed circuit (FPC) with a fabricated three-conductor coplanar transmission line (CTL) is used in

place of a coaxial cable. This choice aims to prevent mechanical breakage of the coaxial cable when subjected to an intense, fast-pulsed magnetic field. This breakage occurs due to a strong inward force on the outer conductor caused by a substantial induction current interacting with the magnetic field. The FPC impedance is designed to be 50Ω to ensure optimal impedance matching for the high-frequency circuit. The central line of the CTL has a hole to hold the substrate of the YBCO thin film, aligned in the $B \parallel \text{CuO}_2$ -plane direction. Fig. 1(b) presents a photograph of the setup around the sample. The CTL transmits the RF signal (RF in) to the sample and carries the reflected RF signal from the sample (RF out). The reflection signal is influenced by the sample's impedance. Consequently, MR can be determined by detecting the magnetic field dependence of the RF signal reflection (output). Similar methods are also discussed in Ref. [26, 27].

The magnetic field components perpendicular to the FPC-plane (B_\perp) generated by the single-turn coil technique cannot be neglected [28], leading to induced electromagnetic noise. Consequently, the position of the FPC is carefully adjusted geometrically to minimize the induced voltage $\partial B_\perp / \partial t$. The three-line CTL offers an advantage in that the voltage measured between the inner and outer conductors is designed not to be affected by $\partial B_\perp / \partial t$. This is achieved because the two closed circuits, consisting of the center and two side lines, generate voltages with opposite signs, allowing cancellation of $\partial B_\perp / \partial t$ effects [26]. The RF output signal is transmitted by a thin but standard coaxial cable connected to the edge of the FPC, where the magnetic field is nearly negligible. To control the temperature from 50 K to 150 K, a liquid helium flux cryostat with a tail part made of plastic is utilized, and the temperature is managed by

controlling the flux flow rate [29].

Results and Discussion. -The raw data of the RF signal reflection at 79 K with its envelope curves are shown as a function of time in Fig. 1(c) together with the magnetic field waveform. The duration time of the magnetic field is approximately $6 \mu\text{s}$, and the obtained maximum field is 103 T. The gray area represents the obtained output signal. The blue lines in Fig. 1(c) represent the envelope curves that show the amplitude of the reflected signal which is extracted from the numerical lock-in technique. At the onset of magnetic field generation, a significant switching electromagnetic noise is unavoidably produced due to the injection of mega-ampere driving electric currents. Consequently, our analysis focuses solely on the data during the field-decreasing process.

By correlating the time scale of the magnetic field $B(t)$ and the amplitude $A(t)$, we obtain the magnetic field dependence of the RF signal amplitude $A(B)$, which is shown in Fig. 2. The $A(B)$ has been measured at varying temperatures (150, 111, 95, 87, 79, 71, 65, and 52 K) up to 103 T. The signal-to-noise (S/N) ratio is improved compared with the previous results [16, 17, 30], in which the transport properties are also investigated with the destructive manner of ultra-high magnetic field generation.

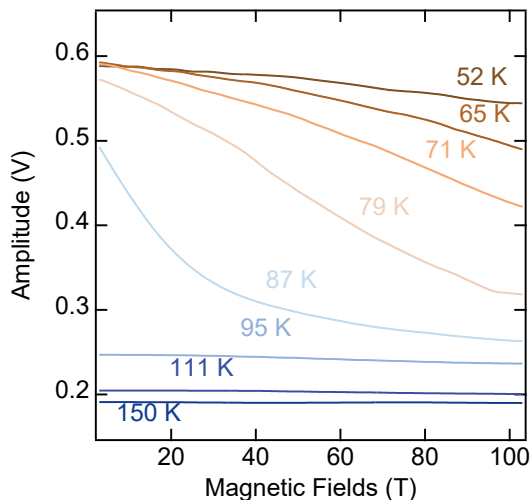


FIG. 2. The magnetic field dependence of the radio frequency reflection amplitude of YBCO for temperatures ranging from 52 K to 150 K up to 103 T.

The temperature dependence of the electrical resistance $R(T)$ as well as the temperature dependence of the RF amplitude $A(T)$ is measured to make the calibration curves $R(A)$. This measurement allows us to experimentally establish a relationship between A and R , rather than obtaining it by analyzing the phase with admittance chart [27]. The calibration curves $R(A)$ are renewed before and after each explosion of single-turn coil

experiment [22], as shown in Fig. S2. This is to reduce the affect of impedance change of the setup caused by the explosion. Thus, by mapping the temperature dependence of A and R , we finally obtain the MR curves $R(B)$ of YBCO via the corresponding transformation from the $A(B)$ in Fig. 2.

The MR curves are exhibited in Fig. 3. The experimental results of MR are successfully measured with a high S/N ratio up to 103 T. Thanks to the utilization of a very thin film (200 nm) and precise alignment, the heating effect of the sample from the magnetic field-induced eddy current is likely to be almost negligible. At 52 K, the resistivity remains nearly constant. At 65, 71, 79, and 87 K, an increase of the resistivity is observed with increasing magnetic field. The kink-structure is observed under certain magnetic fields of 18, 40 and 78 T at 65, 71, and 79 K, respectively, which indicates the onset of the suppression of superconductivity. At temperatures above T_c (95, 111, and 150 K) the MR will likely exhibit a linear behavior concerning B with a small slope.

Observing almost no change in MR at 52 K, it proves that superconductivity persists even up to 103 T without being quenched. In contrast, the suppression of the superconductivity is clearly observed as the positive change of MR in the temperature range from 65 K to 87 K. As the temperature increases, the magnetic field position where the kink in MR appears gradually shifts to lower magnetic fields, disappearing at 95 K when the temperature exceeds T_c (≈ 90 K). The upper critical magnetic field (B_{c2}) is defined as the magnetic field where the resistivity reaches 90% of the resistivity of the normal phase near the superconducting-normal phase transition. This definition aligns closely with the approach outlined in Ref. [30, 31]. The obtained B_{c2} are closely aligned with the phase boundary previously determined using the transmission method in pulsed magnetic field experiments [18, 19] (See in Fig. S3).

In Fig. 3, the MR above T_c (95, 111, 150 K) exhibits an almost linear trend up to 103 T. A similar linear behavior is also observed at 87 K over the highest magnetic field range, indicative of the metallic state. The rate of resistivity increase becomes small around 20 T and remains constant at higher fields, resulting in the B -linear characteristic. However, at 71 K and 65 K, the MR curves show an increasing trend at specific magnetic fields, and the rate of increase does not yet exhibit a constant tendency even in the highest magnetic field region.

To discuss the MR behavior in more detail, we follow the previous work in Ref. [15] and introduce the field slope parameter β ($= d\rho/dB$). We perform the differentiation analysis for each MR and get the field dependent β value, the typical differential curves $d\rho/dB$ at 87 and 79 K are shown in the inset of Fig. 4(a). The β values at high field region around 100 T are plotted in Fig. 4(a). We also show the β value here obtained by the linear fitting of MR in the vicinity of 100 T. The β values ob-

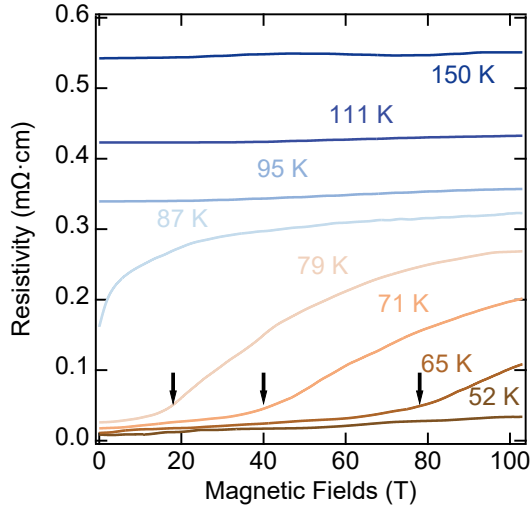


FIG. 3. Magnetoresistance of YBCO for temperatures ranging from 52 K up to 150 K up to 103 T. The arrows indicate the magnetic field positions of the kink structure where the superconductivity starts to be suppressed.

tained by these two methods are relatively close. As the temperature decreases from a high temperature of 150 K, β exhibits a gradual increase in the temperature region higher than T_c and shows a rapid rise near T_c , eventually converging when the temperature is lower than T_c , i.e., 87 and 79 K.

In order to gain a more comprehensive understanding of the temperature-independent behavior of β below T_c , the same analysis is also conducted for the results reported by Miura *et al.* [16]. The experiment done by Miura *et al.* was performed using a YBCO thin film under $B \perp \text{CuO}_2$ -plane up to 50 T. As shown in Fig. 4(b), β converges below T_c , which is similar with our results observed in $B \parallel \text{CuO}_2$ -plane. We note that the T_c (≈ 82 K) of the YBCO thin film in [16] is slightly lower than the thin film used in this work. The similar converged behavior of β below T_c in this work and previous studies indicate that this is a characteristic of the strange metal state independent of the field direction in YBCO.

It should be worth noting that there is a difference of magnitude by a factor of three in the β for two different magnetic field directions, i.e. the converged value of β is about 0.3 and 0.9 $\mu\Omega\text{-cm/T}$ in the $B \parallel \text{CuO}_2$ - and $B \perp \text{CuO}_2$ -plane, respectively. One possible explanation for this numerical difference of β is that the two-dimensionality of the CuO_2 -plane plays an important role in governing the MR properties in the high-field metal phase of YBCO. The orbital effect is less significant and the Zeeman energy dominates the destruction of the Cooper pair in $B \parallel \text{CuO}_2$ -plane, while in $B \perp \text{CuO}_2$ -plane the orbital effect is the major mechanism for the destruction of the superconductivity [19]. After the Cooper pairs

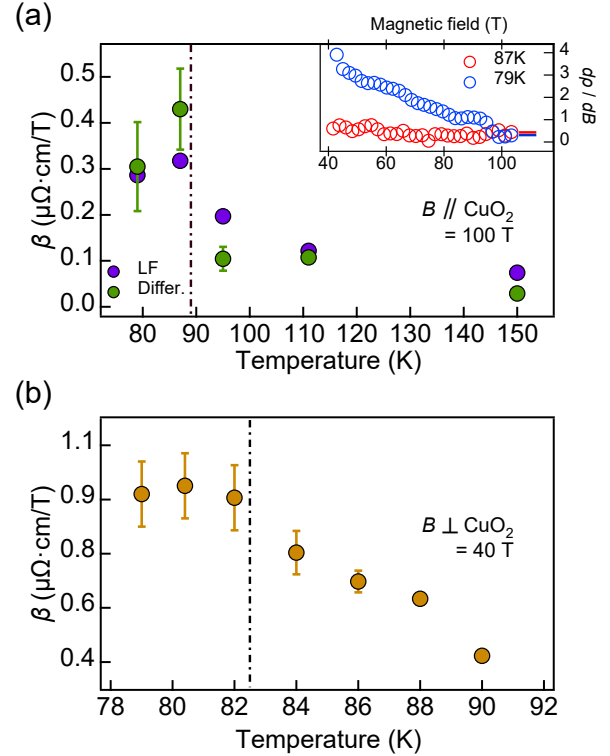


FIG. 4. (a) The variation of field slope parameter β of MR in $B \parallel \text{CuO}_2$ -plane. The green circles represent the differential of MR near 100 T. The detailed $d\rho/dB$ values of MR versus magnetic fields at 87 and 79 K are shown in the inset, in which the horizontal blue and red line represents the average value of $d\rho/dB$ around 100 T for 79 and 87 K, respectively. The purple circles are evaluated from linear fitting (LF), the detailed determination is shown in Fig. S4; (b) The β at $B \perp \text{CuO}_2$ -plane directions obtained from Ref. [16]. The dashed line represents the critical temperature T_c of the YBCO sample.

are broken by the external field, the quantum fluctuation due to the quantum criticality govern the MR and the B -linear behavior appears. Thus, the observed difference of β should result from an anisotropy in the quantum criticality for the strange metal phase that exists above the quantum critical point.

This high-field B -linear behavior in the strange metal phase is also reported in $\text{La}_{2-x}\text{Sr}_x\text{CuO}_4$ (LSCO) [15, 32], $\text{La}_{2-x}\text{Ce}_x\text{CuO}_4$ (LCCO) [14] and even iron pnictide superconductor $\text{BaFe}_2(\text{As}_{1-x}\text{P}_x)_2$ [33]. It is commonly believed that under very high magnetic fields, quantum critical fluctuations, such as nematic and antiferromagnetic fluctuations, play a significant role in determining the properties of HTSCs. These materials exhibit a so-called strange metal state, characterized by strongly correlated behavior and non-Fermi liquid properties [1, 34–38]. Since a similar phenomenon is observed in our work, the quantum critical fluctuation should also be deemed to

be essential in the high magnetic field metal phase in the optimally doped YBCO. The anisotropic β in $B\parallel\text{CuO}_2$ - and $B\perp\text{CuO}_2$ -plane directions is a piece of concrete experimental evidence that the strange metal state is also highly anisotropic. Further theoretical research on the correlation between quantum fluctuations in strange metals and superconducting ground states is required.

Here, we note that the magnetic field of 100 T is not sufficient to break superconductivity at lower temperatures. According to [18], the upper critical magnetic field at 4.2 K in our experiment direction ($B\parallel\text{CuO}_2$ -plane) is about 250 T. The MR at lower temperatures far below T_c is therefore a promising future issue to be clarified. Electromagnetic flux compression [39, 40] is required to generate an ultra-high magnetic field in the range of 1000 T [23] that would be necessary for the future study.

Summary. -We have observed the MR in YBCO at varying temperatures via the RF reflection method in ultra-high magnetic fields exceeding 100 T with the condition of $B\parallel\text{CuO}_2$ -plane. An unconventional linear-in-field (B -linear) MR at a high magnetic field is observed, and the field slope parameter β ($=d\rho/dB$) of MR is converged below T_c . Significantly, this behavior is similar to the previous results of other HTSCs, indicating that it is a common characteristic of HTSCs. This convergence of β suggests that the MR behavior of the field-induced strange metal phase should be determined by the quantum critical fluctuation at high magnetic fields. Thus, the β values under the different directions of the magnetic field indicate the anisotropy in quantum critical fluctuations in the strange metal phase of YBCO. Because there is already substantial evidence indicating that the strange metal phase in high temperatures or high magnetic fields lies in the quantum critical phase of HTSCs, and is closely related to the mechanism of superconductivity in HTSCs [11], the characteristics of β value in our work are also considered to provide significant clues toward a future understanding of the strange metal phase linked with the superconductivity in HTSCs.

Acknowledgement. -S.P. and X.-G.Z. thank for the fruitful discussions with Takashi Shitaokoshi, Yoshimitsu Kohama, Kazuki Matsui and Wei Li. This work was funded by the JSPS KAKENHI, Grant-in-Aid for Transformative Research Areas (A) Nos.23H04859 and 23H04860, Grant-in-Aid for Scientific Research (B) No. 23H01117, and Grant-in-Aid for Challenging Research (Pioneering) No.20K20521. X.-G.Z. and Y.H.M. was funded by JSPS KAKENHI No. 22F22332.

-
- [1] B. Keimer, S. A. Kivelson, M. R. Norman, S. Uchida, and J. Zaanen, From quantum matter to high-temperature superconductivity in copper oxides, *Nature* **518**, 179 (2015).
 [2] S. Sachdev, Colloquium: Order and quantum phase tran-

- sitions in the cuprate superconductors, *Rev. Mod. Phys.* **75**, 913 (2003).
 [3] R. Scanlan, A. Malozemoff, and D. Larbalestier, Superconducting materials for large scale applications, *Proceedings of the IEEE* **92**, 1639 (2004).
 [4] M. Noe and M. Steurer, High-temperature superconductor fault current limiters: concepts, applications, and development status, *Superconductor Science and Technology* **20**, R15 (2007).
 [5] D. Larbalestier, A. Gurevich, D. M. Feldmann, and A. Polyanskii, High- T_c superconducting materials for electric power applications, *Nature* **414**, 368 (2001).
 [6] M. Gurvitch and A. T. Fiory, Resistivity of $\text{La}_{1.825}\text{Sr}_{0.175}\text{CuO}_4$ and $\text{YBa}_2\text{Cu}_3\text{O}_7$ to 1100 K: Absence of saturation and its implications, *Phys. Rev. Lett.* **59**, 1337 (1987).
 [7] P. W. Anderson, Experimental constraints on the theory of high- T_c superconductivity, *Science* **256**, 1526 (1992).
 [8] N. E. Hussey, Phenomenology of the normal state in-plane transport properties of high- T_c cuprates, *Journal of Physics: Condensed Matter* **20**, 123201 (2008).
 [9] P. W. Anderson and Z. Zou, "Normal" Tunneling and "Normal" Transport: Diagnostics for the Resonating-Valence-Bond State, *Phys. Rev. Lett.* **60**, 132 (1988).
 [10] L. B. Ioffe and A. I. Larkin, Gapless fermions and gauge fields in dielectrics, *Phys. Rev. B* **39**, 8988 (1989).
 [11] P. W. Phillips, N. E. Hussey, and P. Abbamonte, Stranger than metals, *Science* **377**, eabh4273 (2022).
 [12] A. Kapitulnik, S. A. Kivelson, and B. Spivak, Colloquium: Anomalous metals: Failed superconductors, *Rev. Mod. Phys.* **91**, 011002 (2019).
 [13] J. Yuan, Q. Chen, K. Jiang, Z. Feng, Z. Lin, H. Yu, G. He, J. Zhang, X. Jiang, X. Zhang, et al., Scaling of the strange-metal scattering in unconventional superconductors, *Nature* **602**, 431 (2022).
 [14] T. Sarkar, P. R. Mandal, N. R. Poniatowski, M. K. Chan, and R. L. Greene, Correlation between scale-invariant normal-state resistivity and superconductivity in an electron-doped cuprate, *Science Advances* **5**, eaav6753 (2019).
 [15] P. Giraldo-Gallo, J. Galvis, Z. Stegen, K. A. Modic, F. Balakirev, J. Betts, X. Lian, C. Moir, S. Riggs, and J. Wu, Scale-invariant magnetoresistance in a cuprate superconductor, *Science* **361**, 479 (2018).
 [16] N. Miura, H. Nakagawa, T. Sekitani, M. Naito, H. Sato, and Y. Enomoto, High-magnetic-field study of high- T_c cuprates, *Physica B: Condensed Matter* **319**, 310 (2002).
 [17] T. Sekitani, Y. Matsuda, S. Ikeda, K. Uchida, F. Herlach, N. Miura, K. Nakao, T. Izumi, S. Tajima, and M. Murakami, Transport measurements of high- T_c superconductors at megagauss magnetic fields by means of a radio frequency transmission technique, *Physica C: Superconductivity* **392**, 116 (2003).
 [18] T. Sekitani, Y. H. Matsuda, and N. Miura, Measurement of the upper critical field of optimally-doped $\text{YBa}_2\text{Cu}_3\text{O}_{7-\delta}$ in megagauss magnetic fields, *New Journal of Physics* **9**, 47 (2007).
 [19] T. Sekitani, N. Miura, S. Ikeda, Y. Matsuda, and Y. Shiohara, Upper critical field for optimally-doped $\text{YBa}_2\text{Cu}_3\text{O}_{7-\delta}$, *Physica B: Condensed Matter* **346**, 319 (2004).
 [20] A. Tsen, B. Hunt, Y. Kim, Z. Yuan, S. Jia, R. Cava, J. Hone, P. Kim, C. Dean, and A. Pasupathy, Nature of the quantum metal in a two-dimensional crystalline

- superconductor, *Nature Physics* **12**, 208 (2016).
- [21] E. Petrenko, L. Omelchenko, A. Terekhov, Y. A. Kolesnichenko, K. Rogacki, D. Sergeyev, and A. Solovjov, Temperature dependence of upper critical fields and coherence lengths for optimally-doped $\text{YBa}_2\text{Cu}_3\text{O}_{7-\delta}$ thin films, *Low Temperature Physics* **48**, 755 (2022).
- [22] N. Miura, Y. Matsuda, K. Uchida, S. Todo, T. Goto, H. Mitamura, T. Osada, and E. Ohmichi, New megagauss laboratory of issp at kashiwa, *Physica B: Condensed Matter* **294-295**, 562 (2001).
- [23] D. Nakamura, A. Ikeda, H. Sawabe, Y. Matsuda, and S. Takeyama, Record indoor magnetic field of 1200 T generated by electromagnetic flux-compression, *Review of Scientific Instruments* **89**, 095106 (2018).
- [24] D. Nakamura, M. M. Altarawneh, and S. Takeyama, Radio frequency self-resonant coil for contactless ac-conductivity in 100 T class ultra-strong pulse magnetic fields, *Measurement Science and Technology* **29**, 035901 (2018).
- [25] P. Mele, K. Matsumoto, T. Horide, O. Miura, A. Ichinose, M. Mukaida, Y. Yoshida, and S. Horii, Tuning of the critical current in $\text{YBa}_2\text{Cu}_3\text{O}_{7-x}$ thin films by controlling the size and density of Y_2O_3 nanoislands on annealed SrTiO_3 substrates, *Superconductor Science and Technology* **19**, 44 (2005).
- [26] B. E. Kane, A. S. Dzurak, G. R. Facer, R. G. Clark, R. P. Starrett, A. Skougarevsky, N. E. Lumpkin, J. S. Brooks, L. W. Engel, N. Miura, H. Yokoi, T. Takamasu, H. Nakagawa, J. D. Goettee, and D. G. Rickel, Measurement instrumentation for electrical transport experiments in extreme pulsed magnetic fields generated by flux compression, *Review of Scientific Instruments* **68**, 3843 (1997).
- [27] T. Shitaokoshi, S. Kawachi, T. Nomura, F. Balakirev, and Y. Kohama, Radio frequency electrical resistance measurement under destructive pulsed magnetic fields, *arXiv preprint arXiv:2306.16277* (2023).
- [28] K. Nakao, F. Herlach, T. Goto, S. Takeyama, T. Sakakibara, and N. Miura, A laboratory instrument for generating magnetic fields over 200 T with single turn coils, *Journal of Physics E: Scientific Instruments* **18**, 1018 (1985).
- [29] Y. H. Matsuda, Y. Kakita, and F. Iga, The temperature dependence of the magnetization process of the kondo insulator YbB_{12} , *Crystals* **10** (2020).
- [30] J. O'Brien, H. Nakagawa, A. Dzurak, R. Clark, B. Kane, N. Lumpkin, R. Starrett, N. Muira, E. Mitchell, and J. Goettee, Experimental determination of the b- t phase diagram of $\text{YBa}_2\text{Cu}_3\text{O}_{7-\delta}$ to 150 T for $B \perp c$, *Physical Review B* **61**, 1584 (2000).
- [31] A. Mackenzie, S. Julian, G. Lonzarich, A. Carrington, S. Hughes, R. Liu, and D. Sinclair, Resistive upper critical field of $\text{Tl}_2\text{Ba}_2\text{CuO}_6$ at low temperatures and high magnetic fields, *Physical review letters* **71**, 1238 (1993).
- [32] R. A. Cooper, Y. Wang, B. Vignolle, O. Lipscombe, S. M. Hayden, Y. Tanabe, T. Adachi, Y. Koike, M. Nohara, and H. Takagi, Anomalous criticality in the electrical resistivity of $\text{La}_{2-x}\text{Sr}_x\text{CuO}_4$, *Science* **323**, 603 (2009).
- [33] I. M. Hayes, R. D. McDonald, N. P. Breznay, T. Helm, P. J. Moll, M. Wartenbe, A. Shekhter, and J. G. Analytis, Scaling between magnetic field and temperature in the high-temperature superconductor $\text{BaFe}_2(\text{As}_{1-x}\text{P}_x)_2$, *Nature Physics* **12**, 916 (2016).
- [34] J. Zaanen, Why the temperature is high, *Nature* **430**, 512 (2004).
- [35] V. Aji and C. M. Varma, Theory of the quantum critical fluctuations in cuprate superconductors, *Phys. Rev. Lett.* **99**, 067003 (2007).
- [36] R. L. Greene, P. R. Mandal, N. R. Poniatowski, and T. Sarkar, The strange metal state of the electron-doped cuprates, *Annual Review of Condensed Matter Physics* **11**, 213 (2020).
- [37] S. Lederer, Y. Schattner, E. Berg, and S. A. Kivelson, Superconductivity and non-fermi liquid behavior near a nematic quantum critical point, *Proceedings of the National Academy of Sciences* **114**, 4905 (2017).
- [38] Z. X. Li, F. Wang, H. Yao, and D. H. Lee, Nature of the effective interaction in electron-doped cuprate superconductors: A sign-problem-free quantum monte carlo study, *Phys. Rev. B* **95**, 214505 (2017).
- [39] E. C. Chare, Magnetic Flux Compression by Magnetically Imploded Metallic Foils, *Journal of Applied Physics* **37**, 3812 (1966).
- [40] B. M. Novac, I. R. Smith, D. F. Rankin, and M. Hubbard, A fast and compact θ -pinch electromagnetic flux-compression generator, *Journal of Physics D: Applied Physics* **37**, 3041 (2004).

Supplementary Materials

A. MORE EXPERIMENTAL DATA

Fundamental properties of YBCO thin film sample

High-quality thin film $\text{YBa}_2\text{Cu}_3\text{O}_7$ are grown by pulsed laser deposition (PLD) method on the SrTiO_3 substrate by Nagoya University. The thickness of the thin film is about 200 nm. Through $2\sigma - \omega$ diffraction pattern measurement, that the YBCO is oriented along the c-axis and the particle mixing ratio in the a-axis is zero percent is confirmed.

The temperature-resistivity curve of the YBCO sample used in this study is shown in Fig. S1. This data was measured in the PPMS (Physical Property Measurement System), and the curves for both the heating and cooling processes show almost no hysteresis. The critical temperature T_c is about 89 K.

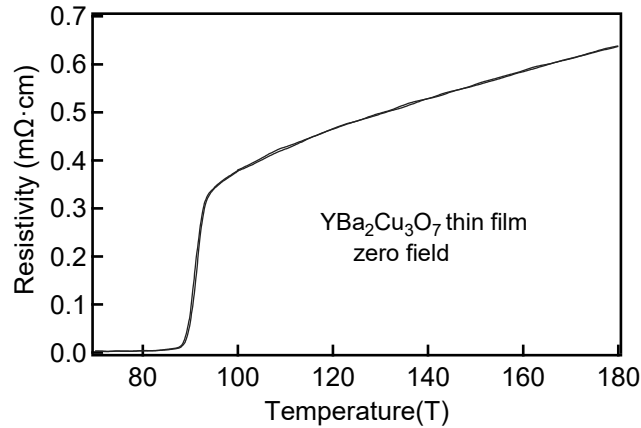


FIG. S1. Temperature dependence of resistivity for YBCO thin film sample used in this study.

Relationship between Amplitude and Resistance

Fig. S2 shows the relationship between amplitude and resistance for each main shot. It should be noted that this relationship has been calibrated before each explosion in a single-turn coil experiment. It is obvious that the amplitude of the RF signal is sensitive around the critical temperature which has a jump of approximately threefold from the superconducting state to the metal state. Thus, it is suitable for investigating the phase transition of YBCO. This transformation is accomplished by mapping the values of amplitude and resistance with temperature dependence in Python.

The critical magnetic fields B_{c2} and the β value obtained in MR curves

Fig. S3 shows the upper critical magnetic field B_{c2} defined as a fixed percentage 90% of the normal phase near the superconducting-normal phase transition, which is the initial part after the slop of MR curves becoming stable as the metal state resistivity value at the temperature of 87, 79 and 71 K. We compare the B_{c2} value with previous research of YBCO in the same magnetic field direction using EMFC [18], which is plotted by a grey triangle in the figure. The upper critical magnetic field B_{c2} obtained in our experimental matches extremely with that obtained by Ref. [18]. Here, we also present how we obtain the β values by linear fitting method in Fig. S4.

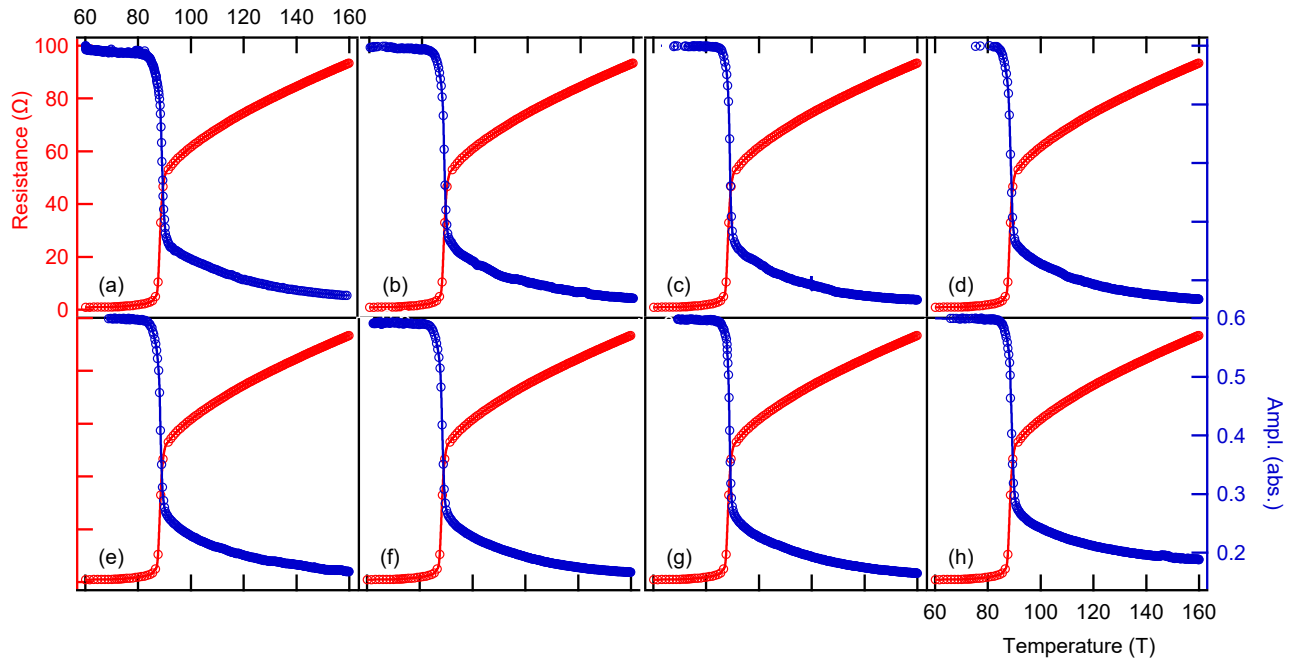


FIG. S2. The relationship between amplitude and resistance before each explosion at (a) 52, (b) 65, (c) 71, (d) 79, (e) 87, (f) 95, (g) 111, and (h) 150 K, respectively.

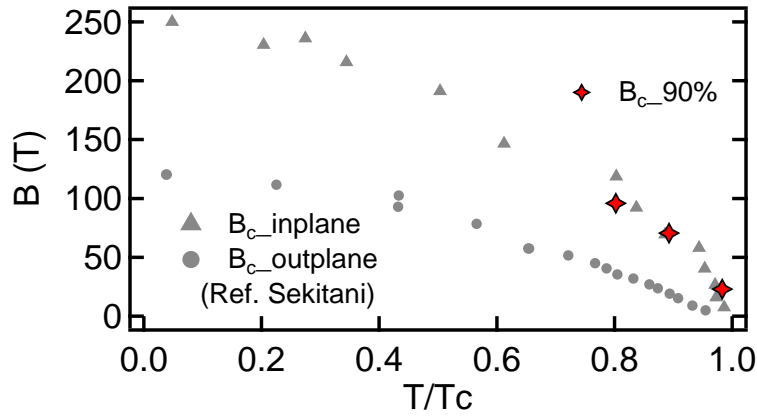


FIG. S3. The upper critical magnetic field B_{c2} defined as a fixed percentage 90% of the normal phase near the superconducting-normal phase transition, which is the initial part after the slop of MR curves becoming stable as the metal state resistivity value at a temperature of 87, 79 and 71 K. For the case at 71 K, the phase transition has not been fully observed, only the starting feature of the saturation is found. The B_{c2} point at 71 K is determined by the extension line of MR guided by the eye at the high field region.

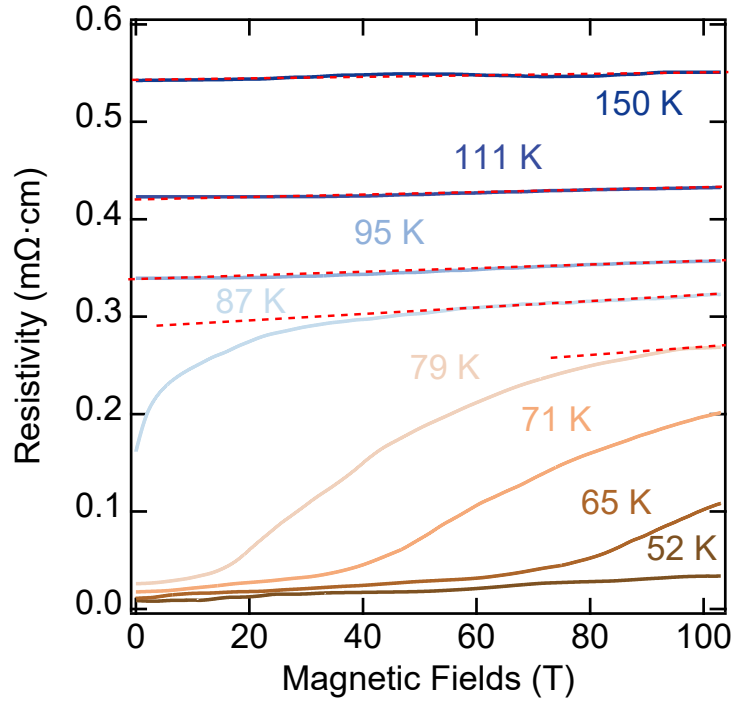


FIG. S4. The MR curves at 87 and 79 K are linearly fit in the highest magnetic field region, while the MR curves above T_c (95, 111, 150 K) are directly fitted in the whole magnetic field region. Then we obtain the magnetic field dependent resistivity $\rho = c + \beta B$, here the β is the field slope whose value is plotted in the Fig. 4(a) as the purple circles.